

# FUDMA Journal of Sciences (FJS) ISSN online: 2616-1370 ISSN print: 2645 - 2944 Vol. 9 No. 11, November, 2025, pp 10 – 26

FJS PROMADORAL OF STREET

DOI: https://doi.org/10.33003/fjs-2025-0911-3893

## INTEGRATED GEOELECTRICAL AND HYDRAULIC CHARACTERIZATION OF BASEMENT AQUIFERS FOR GROUNDWATER EXPLORATION IN KUJE DISTRICT, ABUJA, NIGERIA

#### Ikuemonisan S. Michael, \*Musa O. Kizito, Akpah A. Fabian and Jimoh B. Jacob

Department of Geology, Federal University Lokoja Nigeria.

Correspondence author email: kizito.musa@fulokoja.edu.ng

#### **ABSTRACT**

Basement complex terrain is typically made of hard rocks with limited porosity and permeability, which pose a serious challenge to the groundwater system and resulted in water scarcity even in the study area. Twentynine Vertical Electrical Soundings and Dar-Zarrouk parameters were analyzed to delineate aquifer systems. Topsoil, lateritic clay, weathered basement, fractured basement, and fresh basement comprised the multilayered subsurface structure that was shown by the VES curves. Typical subsurface sequences with alternating resistive and conductive layers reveal weathered or fractured aquifers typical of basement terrains. These curve types include KH-type (41.38%), HA-type (24.15%), KHA (10.35%) and QH (6.90%), H, HK, AK, and HAA ( $\leq$ 3.45%). It was determined that the principal aquifers were the weathered and fractured basement layers, with thicknesses ranging from 3 to 52m and resistivity values between 38.0 and 2429.3 $\Omega$ m. Transverse resistance (250–43,934 $\Omega$ m<sup>2</sup>), hydraulic conductivity (0.3–13m/day), longitudinal conductance (0.01–0.32S), and transmissivity (3.5–161m²/day) were among the Dar Zarrouk parameters that showed significant spatial variability. The northeastern sector (Kuje central) had high-yield zones due to favorable permeability and thickness, while the northwestern and southwestern areas (Chibiri and Godaji area) had limited groundwater potential. The aquifers' rate of pollution is poor to moderate. These findings provide a framework for sustainable groundwater exploration in basement complex terrains.

Keywords: Groundwater, Aquifer Properties, Vulnerability, Abuja, Central Nigeria

#### INTRODUCTION

Water is one of the most important resources for life, modern inventions and the world's population growth are two of the main factors contributing to the increasing demand for water supplies. Therefore, the sustainable use of water resources is essential for the well-being of any society (Sunkari et al., 2021, Musa et al., 2025; Jimoh et al., 2025). Surface water sources include lakes, ponds, dams, springs, rain, streams, and rivers; subsurface water sources include boreholes and handdug wells; groundwater sources are the most reliable and efficient source of potable water (Kizito et al., 2023; Ayedun et al., 2015; Sunkari et al., 2019; 2021), and their contamination poses health risks (Ibrahim et al., 2015; Aminu et al., 2022). Groundwater occurs in sheared bedrock, fractured bedrock, and weathered layers, and its occurrence and accumulation depend on the degree and type of rock fracturing, the thickness and degree of weathering, and the hydrogeological continuity (permeability) of the fractured or weathered zones (Kizito et al., 2023a; Akinwunmiju et al., 2016; Sunkari et al., 2021). Accessing this requires a high level of knowledge and experience (Joel et al., 2020).

The lower Usman Dam in Bwari, Nigeria, supplies surface water to most of the Federal Capital Territory (FCT), including Kuje. However, the dam has not been able to meet the state's water demand, and inhabitant has to resort to use of groundwater. Several investigations have been carried out to investigate the causes of the borehole failures. Among other things, they found that insufficient knowledge of the hydrogeological conditions in the area is one of the causes of the borehole failures (Konwea *et al.*, 2020; Ajayi and Abegunrin, 2022).

Federal Capital Territory (FCT) and some part of the study region and the have been investigated for its groundwater conditions utilizing a variety of hydrogeological, geophysical, and remote sensing techniques. Adeeko and Buba (2016) used Vertical Electrical Sounding (VES) to describe subsurface geoelectric layers and identify worn and cracked basement

aquifers that demonstrated the potential for groundwater development at 35 meters. Mephors et al. (2021) used Digital Elevation Models (DEM) to evaluate groundwater flow directions and elevations, identifying areas with low groundwater potential because of high elevation and rocky terrain. Ejepu et al. (2017) and Ebele & Nur (2020) mapped hydrogeological lineaments and structures aeromagnetic and remote sensing data, finding that fracture density and orientation play a major role in controlling groundwater occurrence. Sunkari et al. (2021) also used VES to identify four distinct geoelectric layers and noted that productive aquifers are primarily located in fractured and weathered basement zones at depths of 40-80 meters, especially in the NE and SE regions of the study area. However, only few have been carried out particularly in the research region by employing single method and concentrates on local assessments which limit the understanding of the groundwater potential of the area. Therefore, the aim of this study is to properly assess and map region's groundwater potential, especially in light of the combined influences of lithology, structural characteristics, aquifer depth, and spatial variability using integrated Vertical Electrical Sounding (VES) and Dar-Zarrouk paramters.

#### **Location of the Study Area**

Kuje is one of the fastest growing towns within the Federal Capital Territory Abuja, North-Central Nigeria. The study area is bounded by latitude of  $8^0$  50'00" to  $8^0$  56'00"N and longitude of  $7^0$  9'00" to  $7^0$ 15'00"E covering a total area of  $130 \text{km}^2$  south west of Abuja, the Capital of Nigeria (Figure 1). Kuje has a total land mass of 1,800sqkrn about (22.5% of FCT) and a population of 97,367 as at the 2006 census, due to urban population growth rate of 4.52% (Jimme *et al.*, 2015). It comprises of two major districts, Kuje central and Rubochi. The area has is a nucleated type of settlement where most of the houses built in the areas depends on the topography of the area due to the presence of hills/mountains surrounding the

area. The study area is accessible through the major highway (Trunk A) connecting Giri junction – Lugbe, with minor road through Gwagwalada-Kuje and other minor roads and foot paths which make the study area accessible for the research purpose. The area comprises of different ethnic groups with varying cultural and social backgrounds namely the Egbirakoto, Gade, Gbari, Gbagyi, Bassa, Hausa-fulani and others. The people are predominantly farmers and traders who specialize in agriculture and livestock breeding. However, other economic activities of the people include trading in pharmaceuticals, provisions, building materials and other essentials such as fruits, vegetables, fresh meat, beans, rice,

fabric, shoes, clothing and smoked fish (Jimme *et al.*, 2015). The area is categorized to be within the guinea savannah belt, even though what we really have now is the derived savannah, only resistant vegetation still remains dominant due to anthropogenic activities of bush clearing and burning, lumbering, most of area consists of secondary regrowth (Jimme *et al.*, 2015). The climate is described as the tropical wet and dry climate of the Koppen's classification. It is characterized by wet and dry season; the rain begins in May and ends in October. With a maximum temperature of 37.9 °C, maximum temperature between December to April (Jimme *et al.*, 2015).

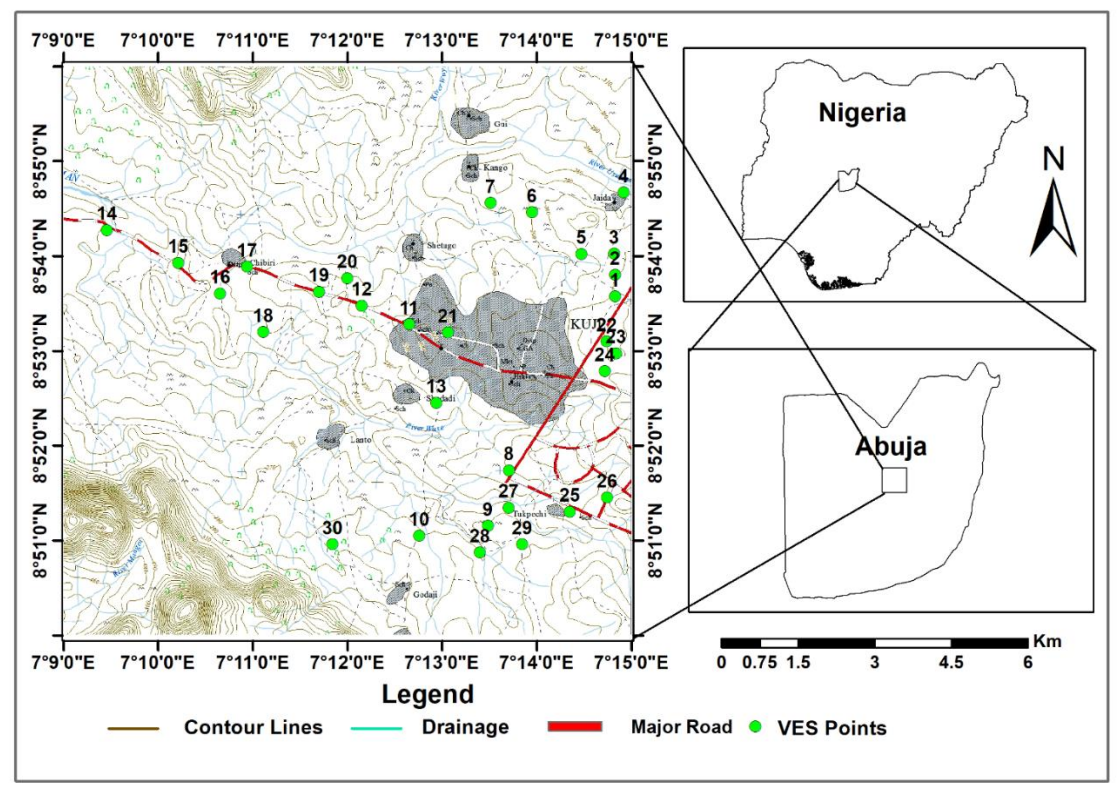


Figure 1: Topographic Map showing the Study Area

#### Geology of the Study Area

The study area is in the south-eastern part of Federal Capital Territory, Abuja which is predominantly underlain by the Precambrian basement complex rocks of Nigeria (Figure 2). The local lithological units in the study area as stated by Ibrahim *et al.* (2015) are biotite granite, biotite and hornblende granite, biotite-hornblende banded gneiss, muscovite schist and migmatite. These rock units occur in a definite pattern within the study area though the migmatite is the widest spread rock unit. They are porphyritic, finely and of medium-coarse-grained texture. Granites mostly occur as intrusive, low-lying outcrops around the gneiss. They are

severely jointed and fairly intruded by quartz veins (Oyawoye, 1964). The soil and geology of Kuje consists of schist, including biotite/muscovite schist muscovite and talc schist with quartz intrusive which accounts for most of the rugged landscape in the area with rocks such as migmatite, granite, gneiss and biotite underlying the region. These geological characteristics pre-dispose the surface soil and land form to slope kinematics such as surface erosion, river bank and mining site landslides and slope failures (Balogun, 2001; Ojigi, 2005; Ojigi et al., 2012; Adeeko and Buba, 2016).

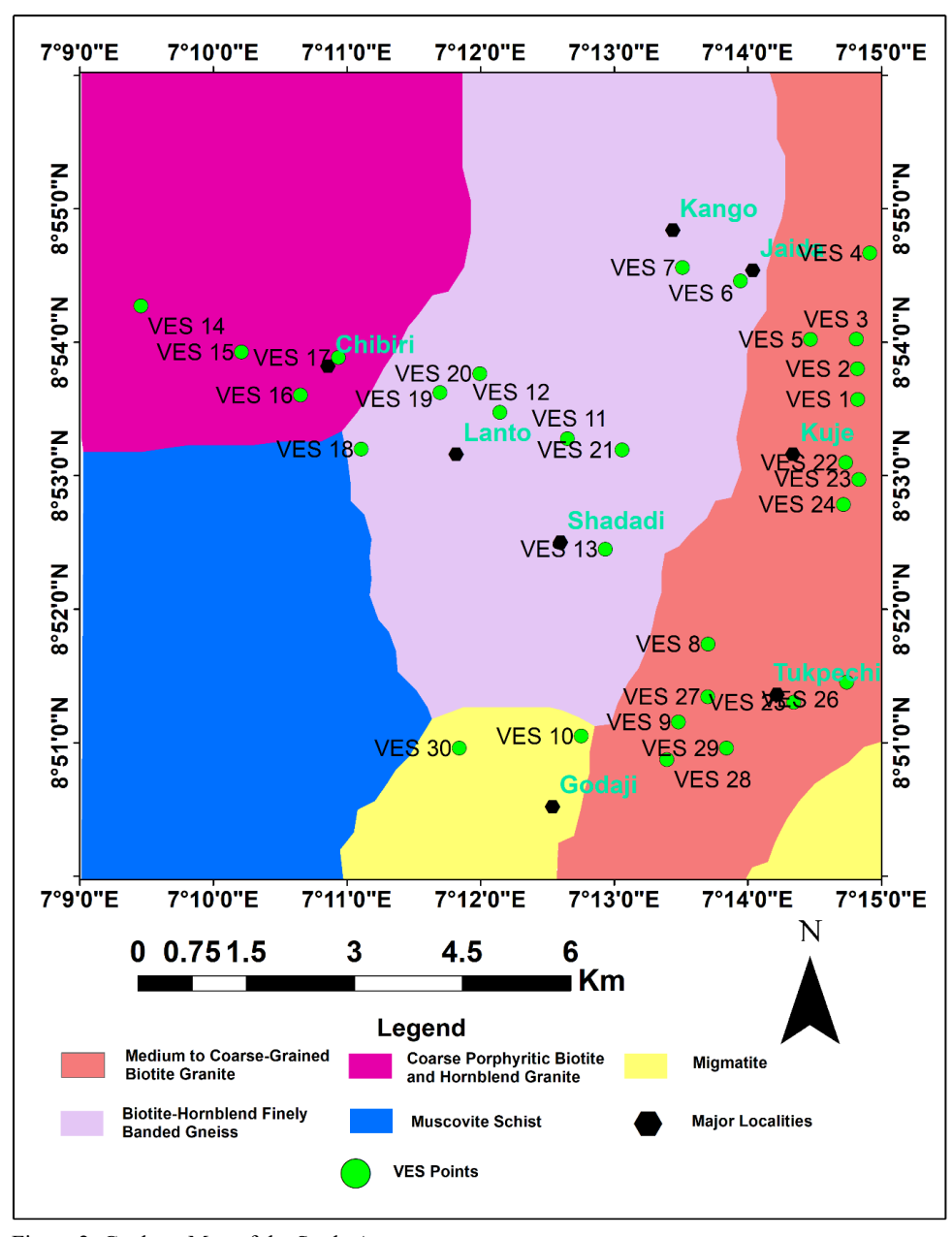


Figure 2: Geology Map of the Study Area

#### MATERIALS AND METHODS Vertical Electrical Sounding

Vertical Electrical Sounding (VES) using the Schlumberger array was conducted at twenty-nine locations within the study area in March 2024 to evaluate subsurface resistivity variations and delineate groundwater-bearing formations. Data acquisition employed a DDR3 digital resistivity meter, four pairs of electrodes, hammers, cable reels, measuring tape, a battery, and a Global Positioning System (GPS). In the Schlumberger array configuration, four steel electrodes (two current and two potential) were aligned linearly, equidistant from the central point of investigation. The current electrodes were progressively expanded outward to increase the depth of investigation, while the potential electrodes were kept fixed until the measured resistance became too small or adjustment was required. Electrode spacing ranged from 1 m to 160 m for current electrodes (AB/2) and 0.5 m to 15 m for potential electrodes (MN/2). The step-by-step electrode arrangement is presented in Table 1. A current of 10–100 amperes was typically injected into the ground. At the end of each sounding, coordinates were recorded (see Table 1), and apparent resistivity values were computed by multiplying the measured resistance (R) with geometric factors derived from standard equations (Equations 1 and 2; Auduson, 2018).

Preliminary interpretation involved manual curve plotting on log-log paper, where apparent resistivity was plotted against current electrode spacing (AB/2). This provided an initial insight into the layering pattern of the subsurface. To enhance accuracy and reduce subjectivity, quantitative modelling was subsequently performed using WinRESIST version 1.0. In this software, resistivity values for each electrode spacing were entered alongside the number of layers, resistivity, and depth estimated from the manual plots. After approximately 30 iterations, the processed data generated interpreted VES curves, delineating subsurface layers with corresponding estimates of resistivity, thickness, and depth. The integration

of manual plotting with iterative computer modelling ensured reliable interpretation of the geoelectric sections. These results form the basis for subsequent analysis of aquifer characteristics, hydrogeological conditions, and groundwater potential in the study area. The final RMS errors for each VES are presented in Table 2. The methodology flow chat is presented in figure 3 below.

$$K = \frac{\pi \left[ \left( \frac{AB}{2} \right)^2 - \left( \frac{MN}{2} \right)^2 \right]}{4 \left( \frac{MN}{2} \right)} \tag{1}$$

$$o_a = KR \tag{2}$$

Where; AB/2 is current electrode spacing, MN/2 is the potential electrode spacing,  $\pi$  is constant,  $\rho_a$  is Apparent resistivity, K is the coefficient of geometric factor, and R is the resistance.

Table 1: Field data Information of the Study Area

S/N	VES No.	Coordinate Northing		Elevation (m)	AB/2 (m)	MN/2 (m)
1	VES 1	08° 53` 34.2``	007° 14` 49.5``	320.3	1.0	0.5
2	VES 2	08° 53` 48``	007° 14` 49.4``	321.0	2.0	0.5
3	VES 3	08° 54`1.3``	007° 14` 48.9``	319.9	3.0	0.5
4	VES 4	08° 54` 40``	007° 14` 54.9``	291.9	6.0	0.5
5	VES 5	08° 54` 1.2``	007° 14` 28.3``	306.3	6.0	1.0
6	VES 6	08°54`27.5``	007° 13` 56.8``	299.5	8.0	1.0
7	VES 7	08° 54` 33.5``	007° 13` 30.8``	293.4	10.0	1.0
8	VES 8	08° 51` 44.2``	007° 13` 42.2``	276.0	10.0	2.5
9	VES 9	08° 51` 09.1``	007° 13` 28.9``	287.0	15.0	2.5
10	VES 10	08° 51` 2.8``	007° 12` 45.3``	278.9	20.0	2.5
11	VES 11	08° 53` 16.6``	007° 12` 39.1``	305.5	30.0	2.5
12	VES 12	08° 53` 28.4``	007° 12` 8.8``	289.5	40.0	2.5
13	VES 13	08° 52` 26.9``	007° 12` 56.1``	285.4	40.0	7.5
14	VES 14	08° 54` 16.2``	007° 09` 27.5``	306.3	50.0	7.5
15	VES 15	08° 53` 55.5``	007° 10` 12.7``	231.2	60.0	7.5
16	VES 16	08° 53` 36.1``	007° 10` 39.2``	249.7	70.0	7.5
17	VES 17	08° 53` 53``	007° 10` 56.2``	256.4	80.0	7.5
18	VES 18	08° 53` 11.8``	007° 11` 6.5``	254.4	80.0	15.0
19	VES 19	08° 53` 37.3``	007° 11` 41.9``	280.1	90.0	15.0
20	VES 20	08° 53` 45.8``	007° 11` 59.7``	277.8	100.0	15.0
21	VES 21	08° 53` 11.5``	007° 13` 3.7``	361.3	120.0	15.0
22	VES 22	08° 53` 5.8``	007° 14` 44.0``	319.6	140.0	15.0
23	VES 23	08° 52` 58.2``	007°14`50.0``	323.0	160.0	15.0
24	VES 24	08° 52` 47.0``	007° 14` 43.1``	330.0		
25	VES 25	08° 51` 18.0``	007° 14` 20.7``	301.3		
26	VES 26	08° 51` 27.0``	007° 14` 44.5``	314.5		
27	VES 27	08° 51` 20.5``	007° 13` 42.1``	282.3		
28	VES 28	08° 50` 52.3``	007° 13` 23.8``	297.6		
29	VES 29	08° 50` 57.4``	007° 13` 50.5``	294.5		

#### **Dar Zarrouk Parameters**

The concept of Dar Zarrouk parameters was first introduced by Maillet (1947). Dar Zarrouk parameters, derived from aquifer resistivity and thickness, were employed to evaluate the hydrogeological characteristics of the subsurface. Specifically, longitudinal conductance (Lc) and transverse unit resistance (Tur) were computed to estimate transmissivity and hydraulic conductivity. The following empirical relationships (equation 3-6) were applied in the calculations as used by various researchers Zohdy et al. (1974), Akpan et al. (2015), Kizito et al. (2023a), (2023b), Hudu et al. (2024), Nanfa et al. (2025):

$$\begin{split} Tur &= h\rho_a \; (\Omega m^2) \\ Lc &= h/\rho_a \; (mho) \end{split} \tag{3} \label{eq:3}$$

$$K = 386.40 \rho_a^{-0.93283} \text{ (m/day)}$$
 (5)  
 $T = Kh \text{ (m}^2/\text{day)}$  (6)

where  $\rho_a$  is aquifer resistivity, h is aquifer thickness, K is hydraulic conductivity, and T is transmissivity. These parameters provide insight into the aquifer's capacity to transmit and store groundwater.

The results for all the parameters including the aquifer resistivity, thickness and depth were contoured using SURFER 25 contouring software from Golden Software Inc., USA. They were gridded using the Kriging method, the choice of the Kriging method was informed by its ability to minimize the variance of the estimation error (Van Beers and Kleijnen, 2003; Jassim and Altaany 2013).

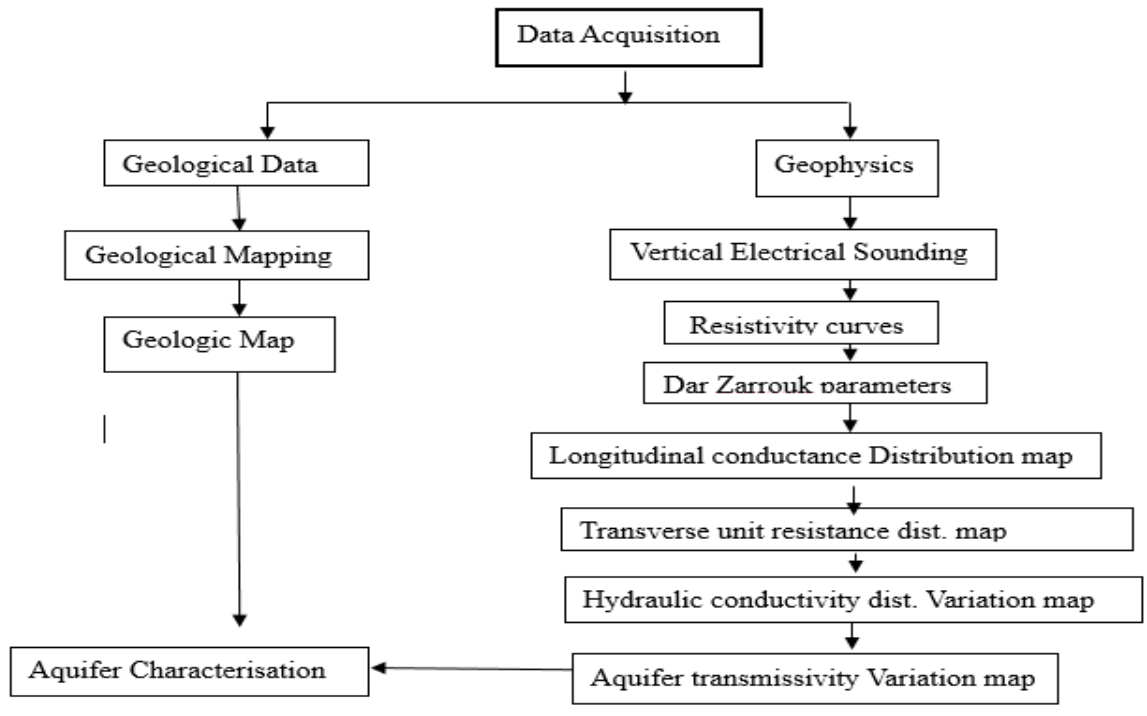


Figure 3: Methodology Flow Chat

#### RESULTS AND DISCUSSION Geoelectrical Layers and its Implication

The computer-based iterative modelling of the sounding curves revealed three- to five-layer earth models comprising topsoil, lateritic clay, weathered basement, fractured basement, and fresh basement (Table 2; Figure 4). The area is predominantly characterized by four-layer curves, in agreement with the works of Aderemi (2020) and Kizito et al. (2023a). The root mean square (RMS) error values ranged from 3.6% to 9.6% (Table 2), which falls within acceptable limits, confirming the reliability of the inversion results. The topsoil constitutes the first geoelectric layer, with resistivity values between 49.4 Ωm and 1037.4 Ωm (average: 543.4  $\Omega$ m). Its thin nature (0.6–3.5 m thick) and variability in resistivity reflect differences in organic matter content. Although not a significant aquifer unit, the topsoil provides important information on near-surface conditions relevant for engineering and soil studies. The lateritic clay layer forms the second unit, showing resistivity values ranging from 1.3 Ωm to 3393.9  $\Omega m$  (average: 1697.6  $\Omega m$ ). Its thickness varies between 2.1 m and 9.6 m, occurring at depths of 2.6-10.8 m. Lateritic horizons often act as semi-confining layers that regulate groundwater recharge. The wide resistivity range observed here suggests heterogeneity in moisture content and degree of lateritization. The weathered basement is a key groundwater-bearing horizon, with resistivity values between 38  $\Omega$ m and 881.6  $\Omega$ m (average: 459.8  $\Omega$ m). Its thickness ranges from 2.7 m to 51.9 m, with depths of 7.7-55.7 m. Low resistivity values indicate significant clay content and low permeability, while higher values imply reduced clay

proportions and enhanced transmissivity. The variation in thickness across the study area reflects differential intensity of bedrock weathering, which directly influences aquifer storage potential. The fractured basement lies beneath the weathered zone and represents an important supplementary aguifer. It has resistivity values ranging from 198.8 Ωm to 2429.3  $\Omega$ m (average: 1314.1  $\Omega$ m), with thicknesses between 10.0 m and 20.9 m, occurring at depths of 32.2-72.6 m. The distinct resistivity contrast and considerable thickness in most locations allowed it to be delineated separately from the weathered zone. Its moderate to high resistivity suggests partial saturation, but zones with relatively lower resistivity are more prospective for groundwater accumulation. The fresh basement is the final unit, characterized by very high resistivity values (>124.7 Ωm, commonly exceeding 1000 Ωm), indicating compact and impermeable bedrock. This unit forms the hydrogeological basement and does not contribute significantly to groundwater storage.

Overall, the resistivity distribution and stratigraphic sequence observed in this study are consistent with findings reported by Osuagwu (2024) and Sunkari et al. (2021). Such agreement underscores the typicality of basement complex terrains, where groundwater occurrence is primarily controlled by the thickness and permeability of the weathered and fractured zones. The close correspondence in apparent resistivity values across studies further validates the reliability of the present geoelectric interpretations. Importantly, the delineated weathered and fractured basement layers represent the most prospective aquifer units within the study area, providing a basis for targeted groundwater exploration and development.

**Table 2: Summary of VES Geoelectric Layer Parameters** 

VES No.	Resistivity	Thickness	Depth	Lithology	Curve Type	RMS Error
VES 1	232.9	3.1	3.1	Top soil	QHA	6.1
	64.6	5.2	8.3	Lateritic clay		
	44.6	7.5	15.8	Weathered Basement		
	198.8	10.0	25.8	Fractured Basement		
	5909.8			Fresh Basement		

VES No.	Resistivity	Thickness	Depth	Lithology	Curve Type	RMS Error
VES 2	226.0	2.6	2.6	Top soil	KH	5.4
	1696.8	6.8	9.4	Lateritic clay		
	268.3	22.3	31.7	Weathered Basement		
TIEG A	7265.9	2.2	2.2	Fresh Basement	***	7.0
VES 3	361.6	2.3	2.3	Top soil	HA	7.9
	49.5	3.4	5.7	Lateritic clay		
	811.6	15.9	21.6	Weathered Basement		
TIEG 4	883.2	1.2	1.0	Fresh Basement	7777	
VES 4	71.5	1.3	1.3	Top soil	KH	5.5
	1199.6	6.1	7.4	Lateritic clay		
	147.3	17.5	24.9	Weathered Basement		
VEC 5	1409.5	0.7	0.7	Fresh Basement	1/11	7.0
VES 5	351.9	0.7	0.7	Top soil	KH	7.0
	1999.8	2.1	2.8	Lateritic clay		
	249.6	26.0	28.8	Weathered Basement		
ATEC (	9598.3	2.6	2.6	Fresh Basement	TTA	7.0
VES 6	325.6	2.6	2.6	Top soil	HA	7.9
	58.0	3.9	6.5	Lateritic clay		
	853.9	20.0	26.6	Weathered Basement		
	587.0	32.0	58.6	Fractured Basement		
VEC 7	2495.7	2.6	2.6	Fresh Basement	TTA	7.2
VES 7	69.9	2.6	2.6	Top soil	HA	7.2
	45.0	2.9	5.5	Lateritic clay		
	85.8	2.7	8.1	Weathered Basement		
	2429.3	12.8	20.9	Fractured Basement		
VEC 0	7477.0	2.2	2.2	Fresh Basement	1.1	0.2
VES 8	359.7	3.3	3.3	Top soil	Н	9.2
	41.0	6.1	9.4	Weathered Basement		
TIEG O	20550.7	1.2	1.2	Fresh Basement	TTA	2.6
VES 9	181.2	1.3	1.3	Top soil	HA	3.6
	83.4	3.4	4.6	Lateritic clay		
	236.3	24.6	29.3	Weathered Basement		
	520.4	22.2	51.4	Fractured Basement		
TIEG 10	2338.1	1.0	1.0	Fresh Basement	TT 4 4	2.7
VES 10	211.1	1.2	1.2	Top soil	HAA	3.7
	1.3	3.8	5.0	Lateritic clay		
	276.7	17.0	22.0	Weathered Basement		
	344.2	17.9	39.9	Fractured Basement		
VEC 11	1302.1	1.6	1.6	Fresh Basement	7777.4	( )
VES 11	347.3	1.6	1.6	Top soil	KHA	6.3
	936.3	5.7	7.3	Lateritic clay		
	153.8	20.3	27.6	Weathered Basement		
	208.1	20.1	47.7	Fractured Basement		
LIEG 12	2375.4	1.0	1.0	Fresh Basement	1/11	<i>5.6</i>
VES 12	126.5	1.0	1.0	Top soil	KH	5.6
	1244.3	5.2	6.2	Lateritic clay		
	363.5	26.3	32.5	Weathered Basement		
VEC 12	4499.0	2.5	2 5	Fresh Basement	A 1/2	4.0
VES 13	109.2	3.5	3.5	Top soil	AK	4.8
	187.4	7.2	10.6	Lateritic clay		
	881.6	22.0	32.6	Weathered Basement		
VEC 14	825.9	1.1	1.1	Fresh Basement	MII	4.2
VES 14	207.2	1.1	1.1	Top soil	KH	4.2
	2452.2	5.3	6.4	Lateritic clay		
	205.2	24.3	30.7	Weathered Basement		
VEC 15	1458.9	1.0	1.0	Fresh Basement	I/ I I A	7.2
VES 15	118.5	1.9	1.9	Top soil	KHA	7.3
	3393.9	8.9	10.8	Lateritic clay		
	520.2	29.6	40.4	Weathered Basement		
	1364.4	32.2	72.6	Fractured Basement		
TIPE 1	3061.2	0.0	0.0	Fresh Basement	TT 4	0.5
VES 16	160.9	0.9	0.9	Top soil	HA	8.5
	39.6	2.3	3.3	Lateritic clay		
	765.3	4.4	7.7	Weathered Basement		
	1886.1			Fresh Basement		

VES No.	Resistivity	Thickness	Depth	Lithology	Curve Type	RMS Error
VES 17	161.6	1.0	1.0	Top soil	KHA	4.8
	448.9	2.6	2.6	Lateritic clay		
	74.7	6.7	10.3	Weathered Basement		
	582.6	15.0	25.4	Fractured Basement		
	1654.6			Fresh Basement		
VES 18	191.9	1.6	1.6	Top soil	KH	9.5
	1366.6	5.0	6.6	Lateritic clay		
	132.3	17.6	24.3	Weathered Basement		
	10520.3			Fresh Basement		
VES 19	205.8	0.6	0.6	Top soil	KH	6.5
	774.3	9.6	10.2	Lateritic clay		
	112.9	16.1	26.3	Weathered Basement		
	3526.6			Fresh Basement		
VES 20	1037.4	0.9	0.9	Top soil	QH	4.6
	233.4	2.2	3.1	Lateritic clay		
	220.3	9.3	12.4	Weathered Basement		
	11366.2			Fresh Basement		
VES 21	49.4	2.1	2.1	Top soil	KH	6.1
	119.2	4.0	6.1	Lateritic clay		
	38.0	11.1	17.2	Weathered Basement		
	4517.1			Fresh Basement		
VES 22	229.2	1.4	1.4	Top soil	KH	3.9
	638.7	4.9	6.3	Lateritic clay		
	323.1	36.3	42.6	Weathered Basement		
	1833.5			Fresh Basement		
VES 23	451.7	1.1	1.1	Top soil	QH	5.7
	121.6	5.4	6.5	Lateritic clay		
	44.3	14.3	20.8	Weathered Basement		
	3908.5			Fresh Basement		
VES 24	260.4	1.6	1.6	Top soil	KH	6.6
	1340.1	6.2	7.8	Lateritic clay		
	130.4	14.6	22.4	Weathered Basement		
	3981.2			Fresh Basement		
VES 25	372.8	1.1	1.1	Top soil	KH	7.0
	1593.8	4.0	5.0	Lateritic clay		
	88.1	14.3	19.3	Weathered Basement		
	8994.9			Fresh Basement		
VES 26	147.2	1.1	1.1	Top soil	KH	7.5
	1795.0	2.9	3.9	Lateritic clay		
	149.0	11.3	15.2	Weathered Basement		
	10593.3			Fresh Basement		
<b>VES 27</b>	389.1	2.5	2.5	Top soil	HK	9.6
	22.9	5.6	8.2	Lateritic clay		
	783.8	30.0	38.2	Weathered Basement		
	124.7			Fresh Basement		
VES 28	191.1	1.0	1.0	Top soil	HA	7.3
	27.4	2.4	3.4	Lateritic clay		
	802.8	43.5	46.9	Weathered Basement		
	1461.2			Fresh Basement		
<b>VES 29</b>	287.4	1.4	1.4	Top soil	HA	6.3
	98.1	2.4	3.8	Lateritic clay		
	297.6	51.9	55.7	Weathered Basement		
	945.0			Fresh Basement		

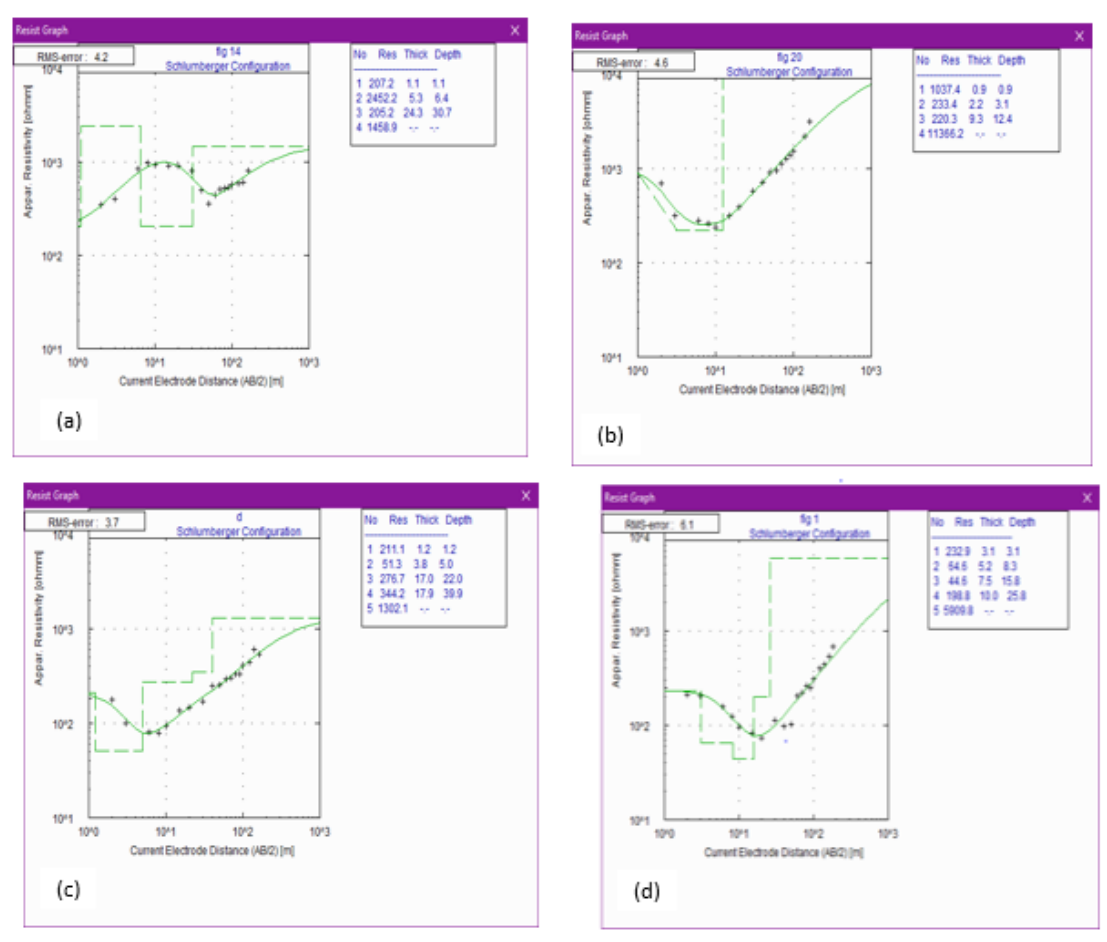


Figure 4: Showing Different Curve Types (a-d) from the Study Area

The VES curve classification in Table 3 and the pie chart distribution in Figure 5 reveals that KH-type (41.38%) and HA-type (24.15%) dominate, indicating common subsurface sequences where alternating resistive and conductive layers suggest weathered or fractured aquifers typical of basement terrains. Less frequent types

like KHA (10.35%) and QH (6.90%) reflect more complex layering, while rare curves (H, HK, AK, HAA;  $\leq$ 3.45% each) point to localized anomalies like thin resistive layers or clayrich zones. This distribution highlights a weathered/fractured aquifer system with variable hydrogeological conditions, guiding groundwater exploration in the region.

S/N	VES curve type	VES No	VES curve characteristic	Freq.	% value
1	QHA	1	$\rho 1 > \rho 2 > \rho 3 < \rho 4 < \rho 5$	1	3.45
2	KH	2, 4, 5, 12, 14, 18, 19, 21, 22, 24, 25, 26,	$\rho 1 < \rho 2 > \rho 3 < \rho 4$	12	41.38
3	HA	3, 6, 7, 9, 16, 28, 29	$\rho$ 1> $\rho$ 2< $\rho$ 3< $\rho$ 4	7	24.15
4	Н	8	$\rho 1 > \rho 2 < \rho 3$	1	3.45
5	KHA	11, 15,17	ρ1< ρ2>ρ3< ρ4< ρ5	3	10.35
6	HK	27	$\rho 1 > \rho 2 < \rho 3 > \rho 4$	1	3.45
7	AK	13	ρ1<ρ2< ρ3> ρ4	1	3.45
8	QH	20, 23	$\rho$ 1> $\rho$ 2> $\rho$ 3< $\rho$ 4	2	6.90
9	HAA	10	$\rho$ 1< $\rho$ 2> $\rho$ 3< $\rho$ 4 <p5< td=""><td>1</td><td>3.45</td></p5<>	1	3.45

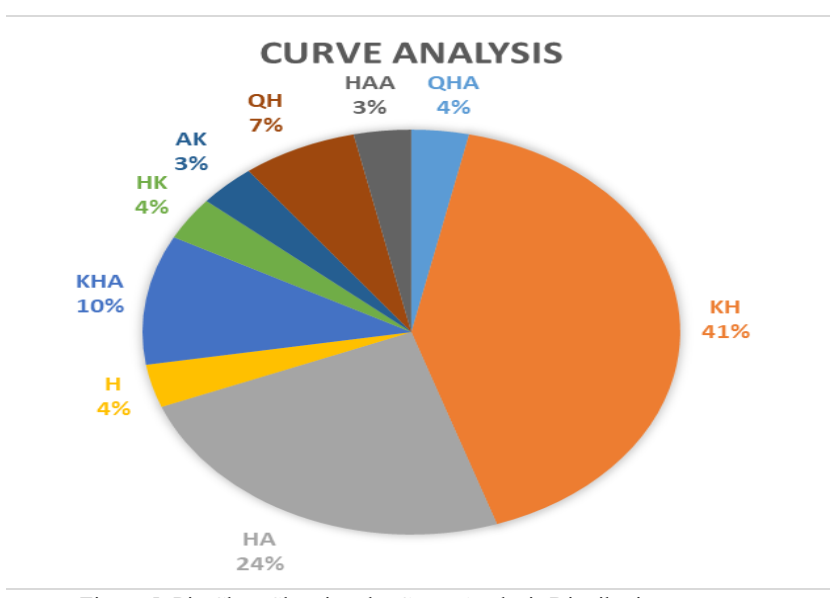


Figure 5: Pie Chart Showing the Curve Analysis Distribution

## Integration of Depth, Resistivity, and Thickness Patterns in Aquiferous Zones

The spatial variation in aquifer characteristics across the study area reveals a clear relationship between depth, resistivity, and thickness in figures 6, 7 and 8 respectively, which has implications for groundwater occurrence and productivity. The depth to the top of the aquifer, represented by the weathered basement layer, ranges from 7.7 m to 55.7 m, yielding an average depth of approximately 31.7 m. The aquifer depth is between 7.7 m and 72.6 m (avg. 31.2 m),

indicating shallow to moderately deep weathered/fractured basement aquifers. The depth map (Figure 6) shows that aquifer zones in the south-eastern sector, particularly near Tukpechi and Kuje, are relatively shallow (4–18 m), while deeper zones exceeding 40 m are found in the north-western and south-central regions. This aligns with Osumeje *et al.* (2024) assertion that thicker aquifers generally offer higher storage and sustainable yields, and such deeper zones may have larger groundwater storage potential.

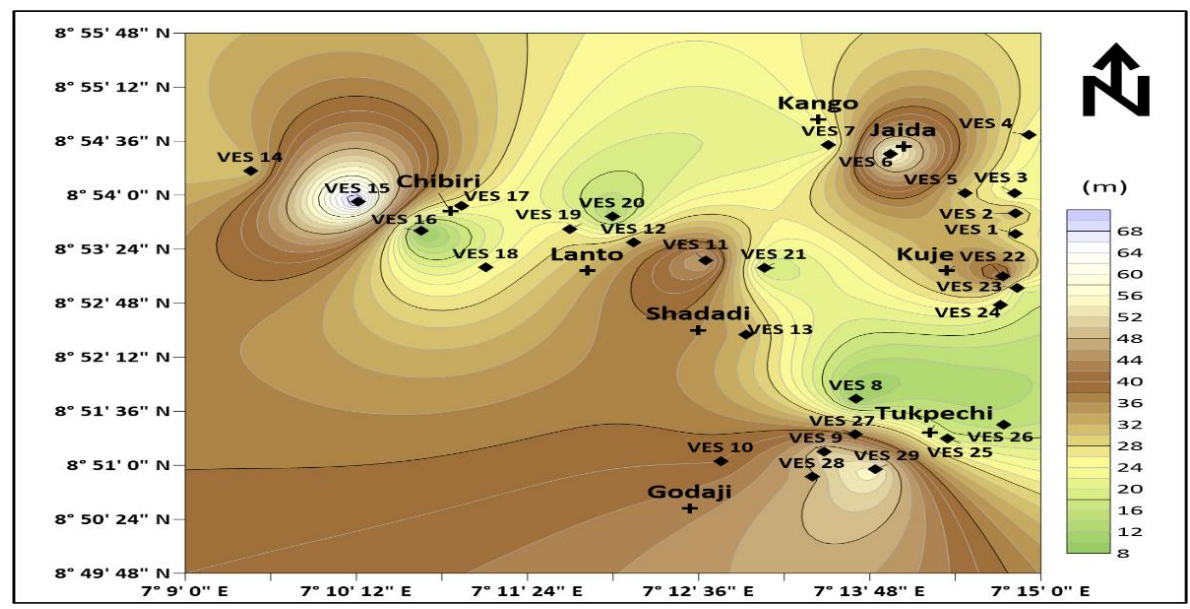


Figure 6: Aquifer Depth Variation Map of the Study Area

The analysis of 29 Vertical Electrical Sounding (VES) points from table 3 revealed significant variations in subsurface resistivity (38.0–2429.3 $\Omega$ m, avg. 451.4 $\Omega$ m), reflecting diverse lithologies from conductive weathered layers to resistive basement rocks. Resistivity distribution map (Figure 7) reveals that the shallow aquifer zones in the south-eastern areas exhibit lower resistivity values (10–60 $\Omega$ m), suggesting the presence of saturated, fine-grained weathered materials or

clayey aquifers. These findings are consistent with Osumeje *et al.* (2024), who noted that thicker aquifers also contribute to better natural filtration, which is critical for reducing the concentration of contaminants. Conversely, higher resistivity values observed in deeper zones, such as Chibiri and Kango, suggest limited groundwater storage in these areas due to the presence of fresh basement or unsaturated weathered materials.

Table 4. Dar	· Zarrouk and	Aquifer Hydra	ulic Parameters	of the Study Area
Table 4. Dai	Zarrouk anu	Addite nvara	une rarameters	or the Study Area

VES No.	P(\Om)	h(m)	d (m)	meters of the Stud Lc (Siemens)	Tur (Ωm²)	K (m/day)	T (m <sup>2</sup> /day)
1	198.8	10.0	25.8	0.05	1988.00	2.77	27.73
2	268.2	22.3	31.7	0.08	5980.86	2.10	46.77
3	811.6	15.9	21.6	0.02	12904.44	0.75	11.87
4	147.3	17.5	24.9	0.12	2577.75	3.67	64.20
5	249.6	26.0	28.8	0.10	6489.60	2.24	58.32
6	587.0	32.0	58.6	0.05	18784.00	1.01	32.32
7	2429.3	12.8	20.9	0.01	31095.04	0.27	3.44
8	41.0	6.1	9.4	0.15	250.10	12.09	73.78
9	520.4	22.2	51.4	0.04	11552.88	1.13	25.09
10	344.2	17.9	39.9	0.05	6161.18	1.66	29.75
11	208.1	20.1	47.7	0.10	4182.81	2.66	53.42
12	363.5	26.3	32.6	0.07	9560.05	1.58	41.54
13	881.6	22.0	32.6	0.02	19395.20	0.69	15.21
14	205.2	24.3	30.7	0.12	4986.36	2.69	65.43
15	1364.4	32.2	72.6	0.02	43933.68	0.46	14.81
16	765.3	4.4	7.7	0.01	3367.32	0.79	3.47
17	582.6	15.0	25.4	0.03	8739.00	1.02	15.26
18	132.3	17.6	24.3	0.13	2328.48	4.05	71.37
19	112.9	16.1	26.3	0.14	1817.69	4.70	75.69
21	38.0	11.1	17.2	0.29	421.80	12.98	144.11
22	323.1	36.3	42.6	0.11	11728.53	1.76	64.00
23	44.3	14.3	20.8	0.32	633.49	11.25	160.90
24	130.4	14.6	22.4	0.11	1903.84	4.11	60.01
25	88.1	14.3	19.3	0.16	1259.83	5.93	84.73
26	149.0	11.3	15.2	0.08	1683.70	3.63	41.01
27	783.8	30.0	38.2	0.04	23514.00	0.77	23.14
28	802.8	43.5	46.9	0.05	34921.80	0.75	32.81
29	297.6	51.9	55.7	0.17	15445.44	1.90	98.79
Minimum	38.0	4.4	7.7	0.01	250.10	0.27	3.44
Maximum	2429.3	51.9	72.6	0.32	43933.68	12.98	160.90
Average	451.4	20.6	31.2	0.09	9988.13	3.17	50.43

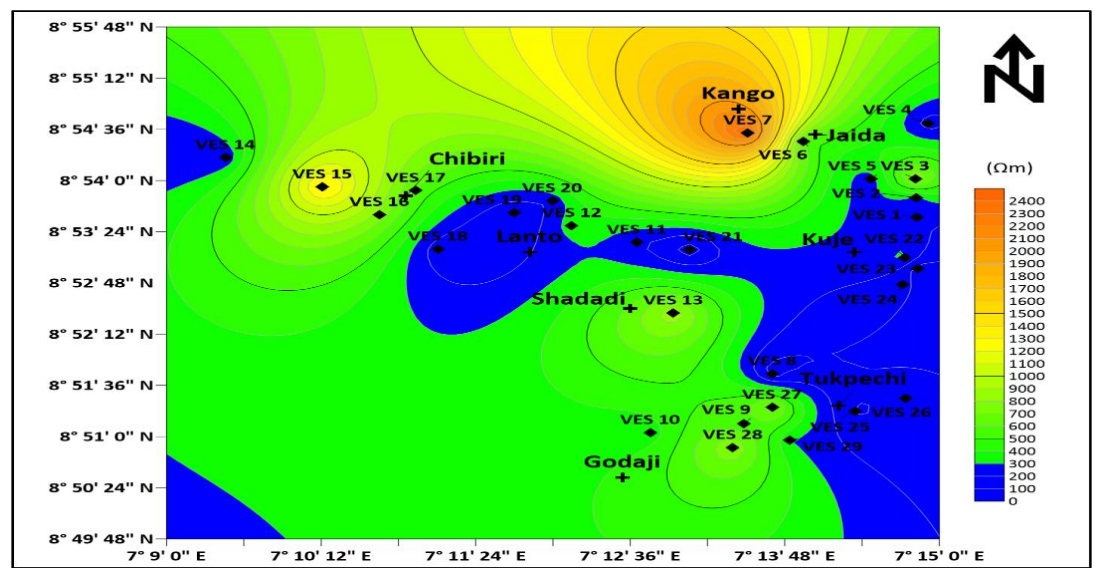


Figure 7: Aquifer Resistivity variation Map of the Study Area

The varying thicknesses of the aquifer layer significantly impact groundwater availability and quality. Thicker aquifers generally offer higher storage capacity and better groundwater quality due to enhanced filtration, while thinner aquifers, although more easily accessible, are more vulnerable to contamination and quicker depletion (Osumeje *et al.*, 2024). Aquifer thickness ranged from 4.4m to 51.9m with an

average value of 20.6 m (Table 4). The thickness map (Figure 8) also indicates that areas with greater aquifer thickness, such as parts of Tukpechi and Godaji, correspond to more favorable groundwater potential. The combination of moderate to high thickness and low to moderate resistivity in the south-eastern sector suggests a favorable environment for groundwater development, in line with the findings of

Osumeje *et al.* (2024) about the importance of aquifer thickness and its role in groundwater sustainability. On the other hand, areas like Chibiri, which exhibit thinner aquifers, may have limited water storage and yield potential. The integration of depth, resistivity, and thickness data suggests that the Tukpechi–Kuje–Godaji corridor represents the most promising groundwater development zone, while areas like

Chibiri and Kango, characterized by high resistivity and low aquifer thickness, are less favorable unless specific fracture zones are targeted. This highlights the critical importance of aquifer characteristics in guiding effective groundwater management strategies, as emphasized by Osumeje *et al.* (2024).

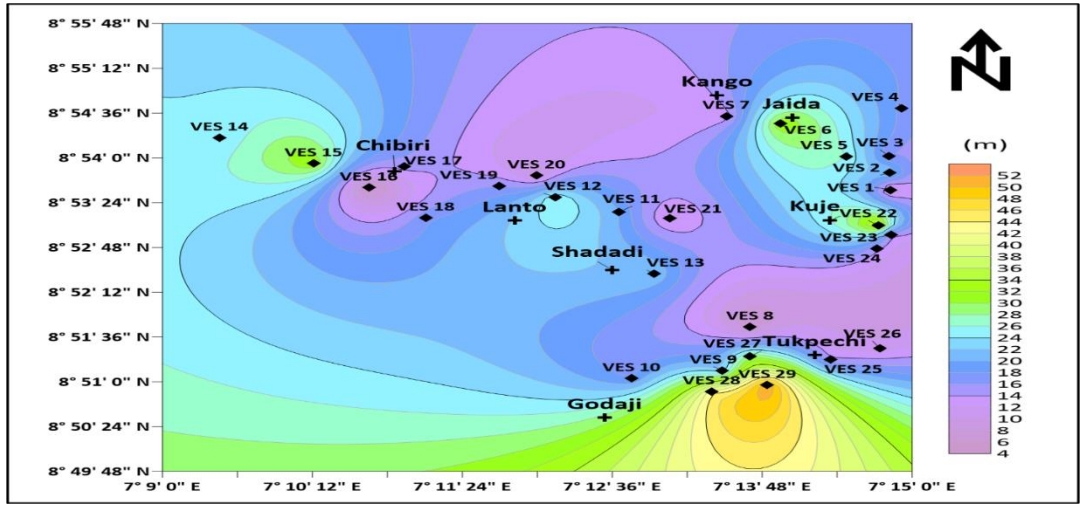


Figure 8: Aquifer Thickness variation Map of the Study Area

## Aquifer Protective Capacity and Groundwater Potential Based on Longitudinal Conductance Variation.

The study area exhibits significant spatial variations in longitudinal conductance (Lc) values, reflecting distinct hydrogeological conditions that influence aquifer protection and groundwater potential (Okonkwo & Ugwu, 2015). The longitudinal conductance value ranges from 0.01-0.32 Siemens with an average value of 0.09 Siemens (Table 4). From the spatial distribution map (Figure 9), the northeastern sector (Kuje area), VES points 21 and 23 demonstrate high longitudinal conductance values ranging from 0.26 to 0.30 Siemens, indicating thick clay-rich weathered layers that provide excellent aquifer protection while facilitating groundwater accumulation in the underlying fractured basement. Moving southeastward (Tukpechi), VES point 25 shows moderate conductance values between 0.18 and 0.22 Siemens, suggesting a mixed clay-sand overburden that offers reasonable protection and moderate groundwater potential. Similar moderate conditions are observed at VES points 14, 22, and 24 in the central-eastern sections, where the weathered profile appears sufficiently developed to support groundwater extraction with proper management. In contrast, the northwestern and southwestern (Kango and Godaji) portions of the study area, particularly at VES points 7, 9, 10, and 16, exhibit concurringly low conductance values below 0.08 Siemens, revealing thin, sandy overburden with minimal protective capacity and high vulnerability to surface contamination. According to Henriet (1976), the ability of an

aquifer to offer protection against contamination is largely influenced by both the thickness and resistivity of the overlying heterogeneous subsurface layers. Consequently, the extent to which groundwater is insulated from potential vertical infiltration of pollutants can be assessed through these parameters. According to the classification system established by Akintorinwa et al. (2020) in table 5, the study area has weak to moderate aquifer protective capacity. The observed spatial patterns align with findings from Simon et al. (2022), who noted that low-conductance zones often correlate with areas of high hydraulic conductivity, creating pathways for potential contaminant infiltration into the groundwater system. This relationship underscores the critical need for comprehensive hydrogeological assessments when planning groundwater development projects in basement complex terrains. The northeastern high-conductance zones emerge as the most promising areas for sustainable groundwater exploitation, combining adequate aquifer protection with favorable storage conditions. Moderate-conductance areas may support localized water supply systems but require careful monitoring to ensure long-term sustainability. The low-conductance zones in the northwestern and southwestern sectors present significant challenges for groundwater development due to their limited protective capacity and uncertain yield potential, though secondary porosity from extensive fracturing could potentially enhance productivity in these areas.

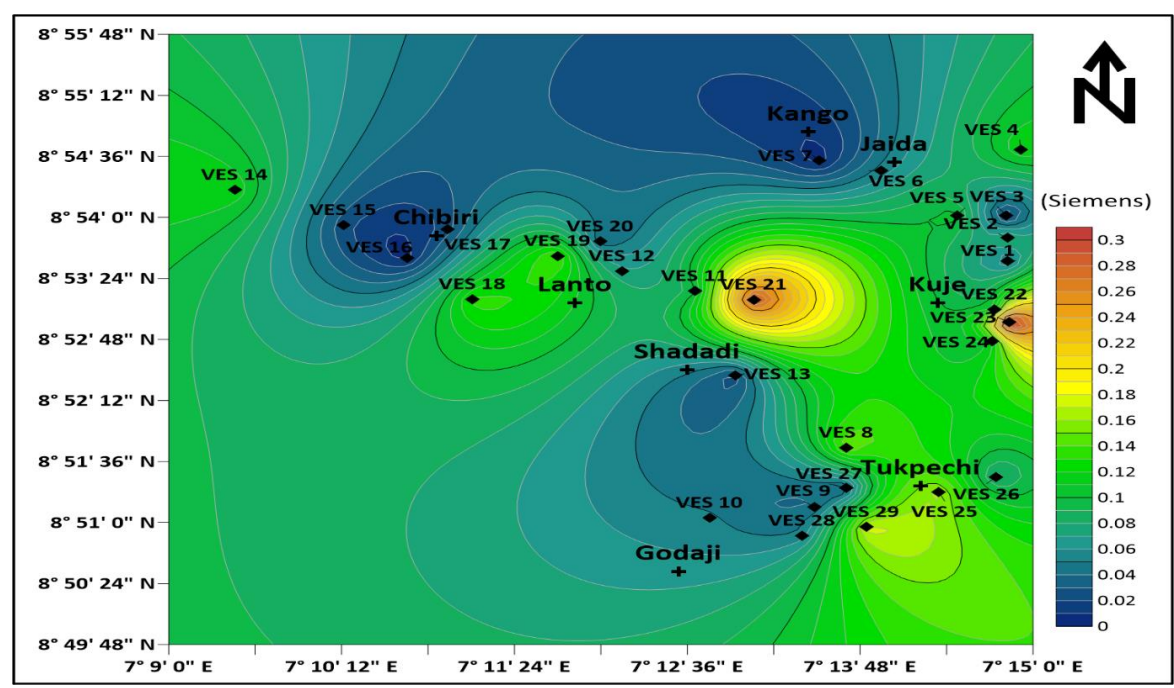


Figure 9: Longitudinal Conductance Distribution Map of the Study Area

Table 5: Aquifer Protective Capacity Rating (Akintorinwa et al., 2020)

S/N	Lc Values	Class
1	< 0.05	weak
2	0.05-1.0	moderate
3	1.0-10.0	good
4	>10	very good

## Spatial Distribution of Transverse Unit Resistance and Its Implications for Groundwater Potential in Basement Complex Terrain

The spatial distribution of transverse unit resistance (TUR) across the study area exhibits significant lateral variations with value ranging from 250.10-43933.68  $\Omega$ m<sup>2</sup> and average value of 9988.13  $\Omega m^2$  (Table 4). This provides valuable insights into aquifer characteristics and groundwater potential. The contour map (Figure 10) reveals particularly high TUR values exceeding 40,000 Ωm² around VES points 15 and 28, which strongly suggest the presence of thick, resistive subsurface units that likely represent well-developed fractured basement zones with substantial saturated thickness. These high-value zones (southwestern and northwestern zones) are considered prime targets for high-yield groundwater abstraction, provided that permeability conditions are favorable. In contrast, significantly lower TUR values below 10,000 Ωm<sup>2</sup> are observed around VES points 8, 24, and 26, indicating potentially thinner aquifer layers or the presence of more conductive lithologies such as clay-rich weathered zones that may limit groundwater potential. Intermediate TUR values found around VES points 7, 13, and 21 represent moderately resistive zones that could support

sustainable groundwater extraction, though their viability depends on complementary hydrogeologic parameters. Zohdy et al. (1974) demonstrated that total transverse unit resistance is a useful indicator for assessing variations in both the thickness and resistivity of subsurface materials. An increase in transverse resistance values typically reflects a corresponding increase in the thickness of high-resistivity formations, as also noted by Kollu et al. (2021). The observed TUR variations demonstrate a clear correlation with the study area's hydrogeological framework, particularly reinforcing the interpretation of spatially heterogeneous aquifer systems. These findings align well with independent hydraulic conductivity and transmissivity analyses, confirming the reliability of TUR as a diagnostic tool in comprehensive aquifer characterization Zones with high groundwater potential are often determined through the evaluation of transverse resistance (Braga et al., 2006; Nejad, 2009; Toto et al., 2008). As demonstrated by Cassiani and Medina (1997), Simon et al. (2022), transverse resistance serves as a key parameter for identifying target areas with good groundwater potential, with the highest values typically corresponding to zones of highest transmissivity in aquiferous formations.

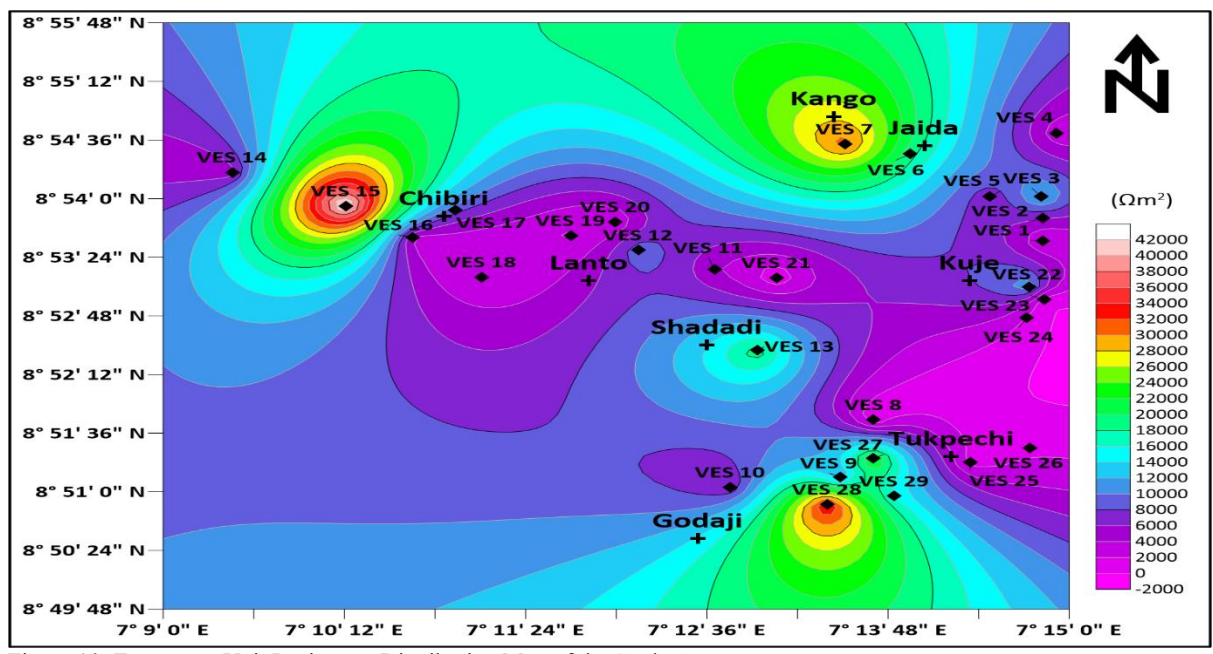


Figure 10: Transverse Unit Resistance Distribution Map of the Study Area

#### Spatial Variability of Aquifer Transmissivity and Groundwater Potential in a Heterogeneous Basement Complex

Transmissivity value ranges from 3.44-169.90 m<sup>2</sup>/day with an average value of 50.43 m<sup>2</sup>/day (Table 4). The spatial distribution map (Figure 11) of transmissivity across the study area exhibits significant lateral heterogeneity, reflecting varying aquifer characteristics and groundwater development potential. The contour map reveals distinct hydrogeological zones, with transmissivity values <20 m²/day to >150 m²/day, demonstrating the complex nature of the subsurface system. High-productivity zones, characterized by transmissivity values exceeding 150 m<sup>2</sup>/day, are predominantly located in the northeastern sector near VES points 21 and 24. These areas, represented by deep red-orange contours on the map, correlate with regions of enhanced aquifer performance, likely resulting from either extensively fractured or weathered basement rocks. Such zones, classified as "High" potential according to Krásný's (1993) classification system, represent optimal targets for sustainable high-yield groundwater abstraction suitable for municipal or agricultural water supply. Moderate transmissivity zones (60-100 m<sup>2</sup>/day), depicted in vellow-green transitions, and are distributed around VES points 13, 22, 25, and 29. These areas fall within Krásný's "Intermediate" productivity category (10-100m<sup>2</sup>/day), indicating aquifers capable of supporting local community water needs and small-scale agricultural operations. The hydraulic characteristics of these zones

suggest the presence of moderately developed fracture networks or weathered materials that can provide reliable groundwater resources with proper management. Conversely, low-productivity areas (northwestern and southwestern sectors), particularly near VES points 7, 10, and 16, exhibit transmissivity values below 20 m²/day (blue-green contours). These zones correspond to Krásný's "Low" to "Very low" productivity categories (1-10m<sup>2</sup>/day and 0.1-1m<sup>2</sup>/day respectively), likely reflecting either clay-rich formations that restrict groundwater flow or thin, poorly developed weathered layers. The observed spatial pattern of transmissivity demonstrates a clear northeast-southwest gradient, with the highest values concentrated in the northeastern and central portions of the study area. This distribution aligns with the regional geological framework, where more intensive weathering and fracturing in the northeast has created more favorable aquifer conditions. The correlation between high transmissivity zones and areas of known basement fracturing supports the interpretation that secondary porosity development is a primary control on groundwater occurrence in this crystalline basement terrain. While no areas in the study reach the "Very high" category (>1000 m²/day). The identified "High" and "Intermediate" zones nevertheless represent significant groundwater resources for regional development. The classification system's utility is particularly evident in distinguishing between areas suitable for different scales of abstraction, from municipal supply to private use.

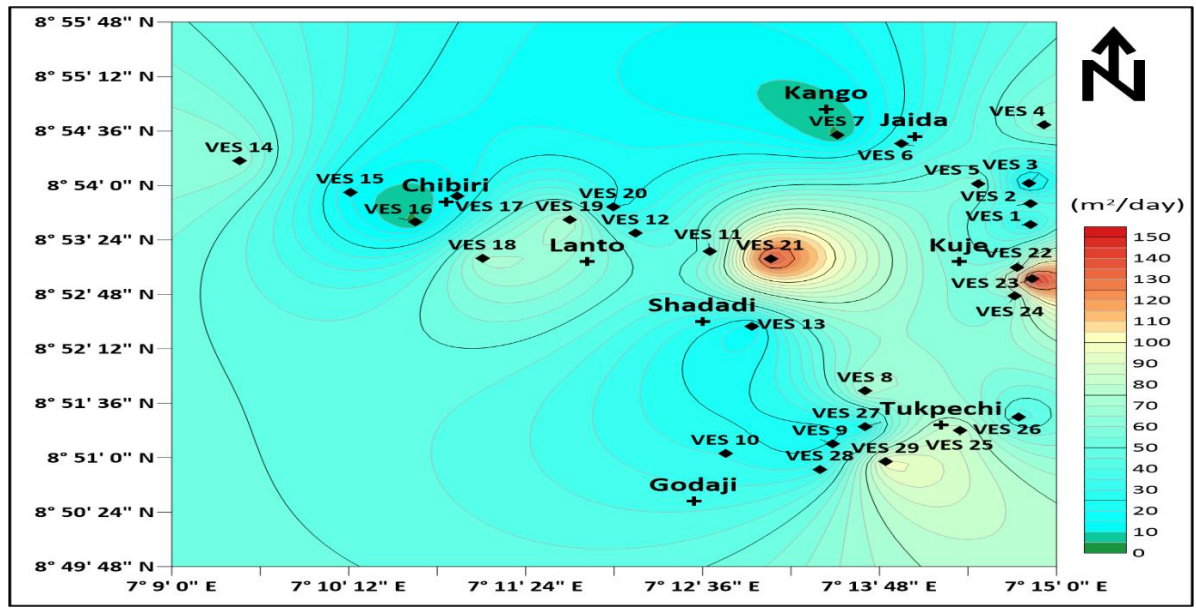


Figure 11: Transmissivity Distribution Map of the Study Area

## Spatial Distribution and Classification of Hydraulic Conductivity in the Study Area

The value of hydraulic conductivity (K) ranges from 0.27-12.98 m/day with an average value of 3.17 m/day (Table 4). The spatial distribution map (Figure 12) of K across the study area reveals significant variability that aligns with the classification system of Singhal and Gupta (1999). The contour map demonstrates distinct hydrogeological zones with K values ranging from <2 m/day to >13 m/day, reflecting varying aquifer characteristics and groundwater potential. High hydraulic conductivity zones (K > 13 m/day), corresponding to Class II ("High") of Singhal and Gupta's (1999) classification, are prominently clustered around VES points 8 and 24. These areas, represented by light blue contours, indicate highly permeable formations such weathered or intensely fractured basement rocks. The elevated K values suggest excellent groundwater flow conditions, making these zones prime targets for high-yield borehole development and efficient aquifer recharge. Moderate conductivity areas (5-10 m/day), falling within the upper range of Class III ("Intermediate") according to Singhal and Gupta (1999), are distributed around VES points 21, 13, and 22. The pale blue to light brown shades on the map suggest formations of mixed lithology, potentially combining sandy layers with finer sediments or moderately fractured basement. While these zones may support sustainable groundwater abstraction, the reduced permeability compared to Class II areas would result in lower optimal pumping rates. Low conductivity zones (K < 2 m/day), classified as Class IV ("Low") in Singhal and Gupta's (1999) system, are concentrated around VES points 7, 16, and 10. The dark brown coloration on the map corresponds to fine-grained materials such as clay-rich layers or compacted weathered rock, which significantly restrict groundwater movement. These areas would require careful consideration for water supply development, as they are likely to yield limited quantities of groundwater. The spatial pattern of hydraulic conductivity demonstrates a clear correlation with the geological framework of the study area. The high-K zones likely represent areas of intense fracturing, while the low-K zones may correspond to clay-filled depressions or zones of reduced weathering. This distribution has important implications for groundwater management, as it directly influences both the potential yield and vulnerability of the aquifer system. There is strong alignment between transmissivity and hydraulic which validates the reliability of the geophysical interpretations. The combination of the two datasets enhances the understanding of subsurface hydrogeologic conditions and supports strategic groundwater exploration and aquifer management.

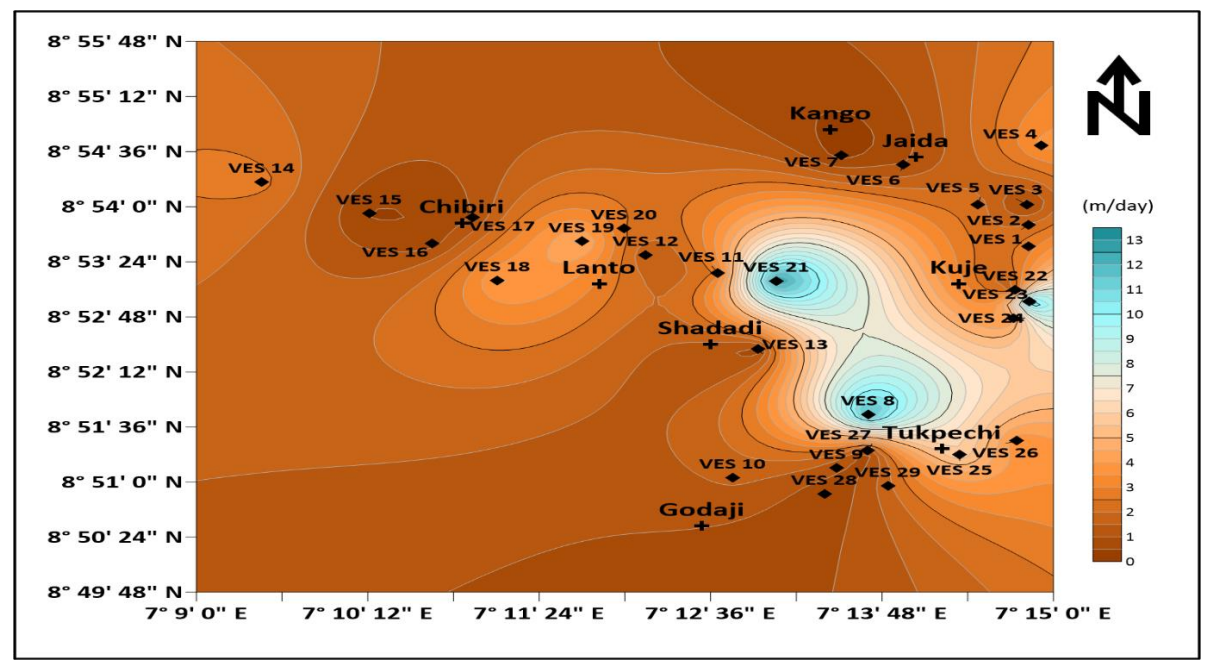


Figure 12: Hydraulic Conductivity Distribution Map of the Study Area

#### **CONCLUSION**

This study employed Vertical Electrical Sounding (VES) and Dar-Zarrouk parameters to evaluate subsurface geoelectric properties and delineate aquifer zones within a basement complex terrain. Analysis of twenty-nine VES points revealed a multi-layered subsurface structure comprising topsoil, lateritic clay, weathered basement, fractured basement, and fresh basement. The weathered and fractured basement layers were identified as the primary aquifers, with resistivity values ranging from 38 to 2429.3 Ωm, thicknesses of 2.7–51.9 m, and depths of 7.7–72.6 m. Thicker aquifers generally provide greater storage capacity and improved water quality, whereas thinner aquifers, though more easily accessible, are prone to contamination and rapid depletion.

Spatial variations in aquifer characteristics were also observed. Shallow aquifer zones in the southeastern sector, particularly near Tukpechi and Kuje (4-18 m depth), exhibited low resistivity values (10-60 \Om), indicating saturated weathered or fractured basement aquifers with favorable groundwater potential. In contrast, deeper zones exceeding 40 m in the northwestern and south-central sectors (e.g., Chibiri and Kango) showed higher resistivity, reflecting limited groundwater storage due to unfractured or unsaturated basement materials. Thickness mapping further highlighted Tukpechi and Godaji as areas with greater aquifer thickness and, consequently, more favorable groundwater prospects. The integration of depth, resistivity, and thickness data indicates that the Tukpechi-Kuje-Godaji corridor represents the most promising zone for groundwater development, while areas such as Chibiri and Kango are less favorable unless boreholes specifically target fracture zones.

The Dar-Zarrouk parameters reinforced these findings. Longitudinal conductance values (0.01–0.32 S) suggest weak to moderate aquifer protective capacity, indicating vulnerability to contamination. Transverse resistance (250.10–43,933.68  $\Omega m^2$ ), hydraulic conductivity (0.27–12.98 m/day), and transmissivity (3.44–169.90 m²/day) provided further insights into aquifer productivity. High transmissivity values (>150 m²/day) in the northeastern sector (VES 21, 23, 24: Kuje, Tukpechi, Shadadi) identified this area as the most suitable for sustainable groundwater abstraction. Conversely,

the northwestern and southwestern regions (VES 7, 10, 16) exhibited low productivity (<20 m²/day), associated with thin, clay-rich layers.

Overall, the results affirm the reliability of geoelectrical methods for groundwater assessment in basement terrains and underscore the importance of integrating geoelectric data with hydraulic parameters for effective resource management. High-potential zones should be prioritized for borehole drilling, while low-yield areas may require alternative water supply solutions or further hydrogeological investigations. Future research should incorporate pumping tests and water quality assessments to validate aquifer performance and ensure long-term groundwater sustainability. This study provides a valuable framework for groundwater resource assessment in basement complex regions and supports informed decision-making by policymakers and water managers. However, borehole logs and pumping test should be carried out for further validation of area with high groundwater potential.

#### REFERENCES

Adeeko, T. O. and Buba, A. A. (2016). Using geo-electrical method of estimation in groundwater for irrigation potentials of Kiyi community, Kuje Area Council, Abuja, Nigeria. *European Journal of Academic Essays*, 3(4), 156-168.

Aderemi, F. L. (2020). Groundwater exploration in a typical basement complex terrain, Southwestern Nigeria. *International Research Journal of Pure and Applied Physics*, 7(1), 1–6.

Ajayi, O. and Abegunrin, O. O. (2022). Borehole failures in crystalline rocks of South-Western Nigeria. *Geology Journal*, 34(4), 397–405.

Akanbi, O. A. (2017). Hydrogeologic characterisation of crystalline basement aquifers of part of Ibarapa area, southwestern Nigeria (Doctoral dissertation).

Akintorinwa O. J., Atitebi M.O., Akinlalu A. A. (2020). Hydrogeophysical and aquifer vulnerability zonation of a

typical Basement Complex Terrain: A case study of Odode Idanre southwestern Nigeria. *Heliyon 6*.

Akinwumiju, A.S., Olorunfemi, M.O., Afolabi, O. (2016). GIS based integrated groundwater potential assessment of Osun drainage basin, southwestern Nigeria. *Ife Journal of Science*, 18(1), 147–168.

Akoteyon, I. S. (2019). Factors affecting household access to water supply in residential areas in parts of Lagos Metropolis, Nigeria. *Bulletin of Geography. Socioeconomic Series*, 43(2019), 7–24.

Akpah F. A., Musa K. O., Shaibu M. M., Nanfa A. C. And Jimoh J. B. (2023). Integration of Vertical Electrical Sounding (VES) Resistivity and Very Low Frequency Electromagnetic (VLF-EM) Methods in groundwater exploration within Ajaokuta and environs, North Central, Nigeria. *FUW Trends in Science & Technology Journal*, 8(2), 269-289.

Akpan, A. E., Ebong, D. E., Emeka N. C. (2015). Exploratory assessment of groundwater vulnerability to pollution in Abi, southeastern Nigeria, using geophysical and geological techniques. *Environmental Monitoring Assessment*, 187, 156.

Aminu, M. B., Nanfa, C. A., Hassan, J. I., Yahuza, I., Christopher, S. D., & Aigbadon, G. O. (2022). Application of electrical resistivity for evaluation of groundwater occurrence within Adankolo Campus and Environs, Lokoja North Central, Nigeria. *European Journal of Environment and Earth Sciences*, 3 (1), 235.

Auduson, A. E. (2018). Concise Applied Geophysics: A Practical Approach. First edition, 2018- In press, University Press PLC, Ibadan, Nigeria.

Ayedun, H., Gbadebo, A. M., Idowu, O. A., & Arowolo, T. A. (2015). Toxic elements in groundwater of Lagos and Ogun States, Southwest, Nigeria and their human health risk assessment. *Environmental monitoring and assessment*, 187, 1-17.

Balogun, O., (2001). The Federal Capital Territory of Nigeria: A Geography of its Development. Ibadan University Press. Pp. 35-37.

Braga, A. C. D. O., Malagutti Filho, W., & Dourado, J. C. (2006). Resistity (DC) method applied to aquifer protection studies. *Revista Brasileira de Geofisica*, 24, 573-581.

Cassiani, G., & Medina, M. A. (1997). Incorporating auxiliary geophysical data into ground-water flow parameter estimation. *Groundwater*, 35(1), 79-91.

Ejepu, J. S., Olasehinde, P., Okhimamhe, A. A., & Okunlola, I. (2017). Investigation of Geological Structures of Hydrogeological Importance of 1: 100,000 Sheet 185 (Paiko) North-Central Nigeria Using Integrated Geophysical and Remote Sensing Techniques. *Preprints*.

Henriet, J. P. (1976). Direct applications of the Dar Zarrouk parameters in ground water surveys. *Geophysical prospecting*, 24(2), 344-353.

Hudu, A. S., Fabian, A. A., Kizito, O. M. and Jacob, B. J. (2024). Application of primary and secondary resistivity parameters in evaluating aquifer potential and vulnerability

within Kabba, North Central Nigeria. FUDMA Journal of Sciences (FJS), 8 (4), 221 – 234.

Ibrahim K. O., Joel O., Abdulrahman A., Bankole S. A. (2015). Physicochemical evaluation of groundwater in Kuje, Federal Capital Territory, Abuja, Nigeria. *Nigerian Journal of Technological Development*, 12(1), 1-5.

Jassim, F. A., & Altaany, F. A. (2013). Image interpolation using Kriging technique for spatial data. *Canadian Journal on Image Processing and Computer Vision*, 4(2), 16–21.

Jimoh, J.B., Musa, O.K, Ahmed II J.B. (2025). An Integrated method for mapping groundwater potential in part of Abuja, Central Nigeria. *Scientia Africana*, 24(1), 339-362.

Joel, E. S., Olasehinde, P. I., Adagunodo, T. A., Omeje, M., Oha, I., Akinyemi, M. L., & Olawole, O. C. (2020). Geoinvestigation on groundwater control in some parts of Ogun state using data from Shuttle Radar Topography Mission and vertical electrical soundings. *Heliyon*, 6(1).

Kizito, O.M., Ahmed II, J.B., Fabian, A.A., Ernest, O.A., Ikenna, A.O., Solomon, S. J., Andrew, C. N., Jacob, B.J. (2023a): Assessment of groundwater potential and aquifer characteristics using inverted resistivity and pumping test data within Lokoja area, North-Central Nigeria. *Communication in physical sciences*, 9 (3), 336 – 349.

Kizito, O.M., Ikenna, A.O., Aaron, E. A., Solomon, S. J., Ernest, O. A., Fabian, A.A, Jacob, B. J. (2023b). Integrating geoelectrical and borehole data in the characterization of basement-rock aquifers in the Lokoja area, Northcentral Nigeria. *Geosystems and Geoenvironment* 2, 10 (02) 17.

Kollu, U., Rao, B. M., Sduarshan, R., Reddy, P. C., & Goud, N. S. (2021). Evaluation of Dar Zarrouk parameters in hard rock terrain in parts of Nuthankal Mandal, Suryapet district, Telangana, India. *Int J Eng Sci Invent*, 10(12), 10-26.

Konwea. C. I., Ajayi, J. O., Bakare, T. A. (2020). Performance of Boreholes and Hand-Dug Wells in The Crystalline Rocks of Osun State, Southwestern Nigeria. *International Journal of Scientific and Technology Research*, 9(1), 3408–3418.

Krásný, J. (1993). Classification of transmissivity magnitude and variation. *Groundwater*, 31(2), 230-236.

Maillet, R. (1947). The fundamental equations of electric prospecting. *Geophysics*, 12, 529–556.

Mephors, J. O., Ogunmuyiwa, C. O., Afolabi, O. S., Agbor, C. F., Ogoliegbune, O. M., Ofordu, C. S. (2021). Use of digital elevation models to map out the groundwater resources base of Kuje area to Federal Capital Territory, Abuja, Nigeria. *Journal of Applied Science and Environmental Management*, 25(7), 1207-1212.

Musa, K. O., Ibrahim, A., Aigbadon, G. O., Akudo, E. O., Akakuru, O., Akpah, F. A., Jacob, B. J., Moses, A., & Baba Aminu, M. A. (2025). Integration of geological and geophysical techniques in groundwater mapping within Lokoja–Jakura schist belt, North Central, Nigeria. *World Journal of Engineering*.

Nanfa, C. A., Musa, O. K., Akpah, F. A., Shaibu, M. M., Jimoh, J. B., Baba Aminu, M., John, O. W., Faith, F. O.,

Rebecca, J. A. and Samson, A. A. (2025). Investigation of basement aquifer hydraulics and protective capacity within Jimgbe and environs, North Central Nigeria. *Communication in Physical Sciences*, 12(2) 696-709.

Nejad, H. T. (2009). Geoelectric investigation of the aquifer characteristics and groundwater potential in Behbahan Azad University Farm, Khuzestan Province, Iran.

Ogunkoya, O.O. (2017). Obafemi Awolowo University Ile-Ife Water Supply Challenges. *Department of Geography*, 71, 2017.

Ojigi, M. L., (2005). Digital Terrain Modeling and Drainage Analysis of Northern Part of Abuja Phase II Development Area, Using Geospatial Techniques. A PhD. Dissertation in Applied Remote Sensing, Fed. Univ. of Tech., Minna, Nigeria. May 2005, 178pg.

Ojigi, M. L., Achema, E. A. and Alade, T. A. (2012) Geospatial Analysis of Landslide Vulnerability in Kuje and Environs, Abuja Nigeria In: Laryea, S., Agyepong, S.A., Leiringer, R. and Hughes, W. (Eds) Procs 4th West Africa Built Environment Research (WABER) Conference, 24-26 July 2012, Abuja, Nigeria, 1067-1077.

Okonkwo, A. C., & Ugwu, G. Z. (2015). Determination of Dar-zarrouk parameters for prediction of Aquifer protective capacity: A case of Agbani Sandstone Aquifer, Enugu State, Southeastern Nigeria. *International Research Journal of Geology and Mining*, 5(2), 12-19.

Osumeje, J. O., Eshimiakhe, D., Oniku, A. S., & Lawal, K. M. (2024). Application of remote sensing and electrical resistivity technique for delineating groundwater potential in North Western Nigeria. Scientific Reports, 14(1), 22299. Oyawoye, M. O. (1972). The basement complex of Nigeria. *African geology*, 67-99.

Shiru et al., (2020): Challenges in water resources of Lagos mega city of Nigeria in the context of climate change. *Journal of Water and Climate Change*, 11(4), 1067–1083.

Simon, S. S., Ishaku, J. M., Seli, A. B., & Boniface, F. (2022). Evaluation of groundwater potentials using Dar Zarrouk parameters in Mapeo and Environs, North-Eastern Nigeria. *Dutse Journal of Pure and Applied Sciences*, 8(3b), 124-135.

Singhal, B. B. S., & Gupta, R. P. (2010). Applied hydrogeology of fractured rocks. *Springer Science & Business Media*.

Sunkari, E. D., Abu, M., Bayowobie, P. S., & Dokuz, U. E. (2019). Hydrogeochemical appraisal of groundwater quality in the Ga west municipality, Ghana: Implication for domestic and irrigation purposes. *Groundwater for Sustainable Development*, 8, 501-511.

Sunkari, E. D., Kore, B. M., & Abioui, M. (2021). Hydrogeophysical appraisal of groundwater potential in the fractured basement aquifer of the federal capital territory, Abuja, Nigeria. *Results in Geophysical Sciences*, 5, 100012.

Talabi, A. O. (2018). Estimated volume of water in shallow wells of Ekiti State, Southwestern Nigeria: implications on groundwater sustainability. *Arabian Journal of Geosciences*, 11(21), 681.

Toto, E. A., Kerrouri, C., Zouhri, L., Basri, M. E., Ibenbrahim, A., Mohamad, H., & Benammi, M. (2008). Geoelectrical exploration for groundwater in Al Maha Forest, Ain Jouhra, Morocco. *Hydrological Processes: An International Journal*, 22(11), 1675-1686.

Van Beers, W. C. M., & Kleijnen, J. P. C. (2003). Kriging for interpolation in random simulation. *Journal of Operational Research Society*, 54,255–262.

Zohdy, A. A., Eaton, G. P., & Mabey, D. R. (1974). Application of Surface Geophysics to Ground-water Investigations: Techniques of Water Resources Investigations of the United States Geological Survey: Book 2: Collection of Environmental Data: Chapter D1. United States Department of the Interior.



©2025 This is an Open Access article distributed under the terms of the Creative Commons Attribution 4.0 International license viewed via <a href="https://creativecommons.org/licenses/by/4.0/">https://creativecommons.org/licenses/by/4.0/</a> which permits unrestricted use, distribution, and reproduction in any medium, provided the original work is cited appropriately.